

Skewness in CMB temperature fluctuations from curved cosmic (super-)strings

Daisuke Yamauchi¹, Yuuiti Sendouda¹, Chul-Moon Yoo^{1,2}, Keitaro Takahashi³,
Atsushi Naruko¹, Misao Sasaki¹

¹*Yukawa Institute for Theoretical Physics, Kyoto University, Kyoto 606-8502, Japan*

²*Asia Pacific Center for Theoretical Physics, Pohang University of Science and Technology, Pohang 790-784, Korea*

³*Department of Physics and Astrophysics, Nagoya University, Nagoya 494-8602, Japan*

E-mail: yamauchi@yukawa.kyoto-u.ac.jp, sendouda@yukawa.kyoto-u.ac.jp,
yoo@yukawa.kyoto-u.ac.jp, keitaro@phys.nagoya-u.ac.jp,
naruko@yukawa.kyoto-u.ac.jp, misao@yukawa.kyoto-u.ac.jp

ABSTRACT:

We compute the one-point probability distribution function of small-angle cosmic microwave background temperature fluctuations due to curved cosmic (super-)strings with a simple model of string network by performing Monte Carlo simulations. Taking into account of the correlation between the curvature and the velocity of string segments, there appear non-Gaussian features, specifically non-Gaussian tails and a skewness, in the one-point pdf. The obtained sample skewness for the conventional field-theoretic cosmic strings is $g_1 \approx -0.14$, which is consistent with the result reported by Fraisse et al. [1]. We also discuss the dependence of the pdf on the intercommuting probability. We find that the standard deviation of the Gaussian part increases and non-Gaussian features are suppressed as the intercommuting probability decreases. For sufficiently small intercommuting probability, the skewness is given by $\lesssim (\text{a few}) \times 10^{-2}$.

KEYWORDS: non-Gaussianity, cosmic strings, domain walls, monopoles.

Contents

1. Introduction	1
2. An analytic model of the string network	3
3. CMB Temperature Fluctuations	5
3.1 The Hindmarsh-Stebbins-Veeraraghavan formula	5
3.2 The Gott-Kaiser-Stebbins effect	7
3.3 Correlations as sources of the skewness	8
3.3.1 Correlation due to cosmic expansion	9
3.3.2 Light-cone effect	9
4. Monte Carlo simulations for the one-point pdf	10
4.1 Setup	10
4.1.1 Scattering probability	10
4.1.2 Assumptions and the expansion of the HSV formula	10
4.1.3 Degrees of freedom of a string configuration	11
4.2 Numerical Results	12
5. Summary	14
A. Reduction of the HSV formula	17
B. Random Variables	18

1. Introduction

Cosmic strings are line-like topological defects formed in the early universe through a spontaneous symmetry breakdown. It was claimed that the formation of cosmic strings at the end of inflation is a generic feature of supersymmetric grand unified theories [2]. The string tension μ is directly related to the symmetry breaking energy scale. Also recent studies of stringy cosmology have revived interest in cosmic strings, because it was pointed out that brane inflation models may produce another class of string objects, called cosmic superstrings [3, 4, 5, 6]. Cosmic superstrings may have different properties from those of conventional field-theoretic cosmic strings. One of the observationally interesting differences is the intercommuting probability P . It can be significantly smaller than unity for cosmic superstrings [7], while normally $P = 1$ for field-theoretic strings [8] (but see [9]).

The imprint of cosmic strings on the cosmic microwave background (CMB) has been widely studied. Although cosmic strings were excluded as a dominant source of the observed

large angular scale anisotropy [10, 11, 12] (see also [13] for a review), a signal due to cosmic strings could still be observed at small angular scales [1, 10] with future arcminutes experiments such as South Pole Telescope [14] or Atacama Cosmology Telescope [15]. On small angular scales, the primary fluctuations are damped and only the integrated Sachs-Wolfe (ISW) effect is relevant. The Gott-Kaiser-Stebbins (GKS) effect [16, 17] is the most characteristic signal of the ISW effect due to cosmic strings. The GKS effect is caused by a discontinuity of the gravitational potential across a moving string segment when photons pass by the moving string. If photons are scattered by a number of moving string segments, the observed temperature fluctuations appear as a superposition of the discontinuities.

Since the network of strings is a highly nonlinear object, its non-Gaussian features may help us distinguish cosmic string signals from other secondary effects and hence may enhance the observability. A skewness, which is a measure of the asymmetry of a probability distribution function, is one of the simplest features of non-Gaussianity [18]. The skewness of temperature fluctuations is defined by

$$g_1 = \frac{\overline{(\Delta - \bar{\Delta})^3}}{\sigma_\Delta^3}, \quad (1.1)$$

where $\Delta \equiv (T - \bar{T})/T = \Delta T/T$, the bar “ $-$ ” denotes the statistical average over a CMB map and σ_Δ the standard deviation. Recently, Fraisse et al. [1] found that the one-point probability distribution function (pdf) of the temperature fluctuations due to conventional cosmic strings has non-Gaussian tails and a negative skewness, $g_1 \approx -0.23$.

Non-Gaussian features would also appear in the bispectrum [19]. Some authors [20, 21, 22] calculated the bispectrum and the trispectrum by using the formula derived by Hindmarsh [23]. In particular, Hindmarsh et al. [20] pointed out that the numerically measured amplitude corresponds to a $|f_{\text{NL}}| \approx 10^3$ for the local-type of primordial non-Gaussianity.

In [24], we computed analytically the one-point pdf of small-scale temperature fluctuations with a simple model of long straight segments and kinks. We derived basic equations for the evolution of string segments in cosmological backgrounds by extending the velocity-dependent one-scale model with the intercommuting probability $P \neq 1$ [24, 25, 26, 27]. It was found that the obtained one-point pdf consists of a Gaussian component due to frequent scatterings by long straight segments and non-Gaussian tails due to close encounters with kinks. The dispersion of the Gaussian component is consistent with the result in [1] and the non-Gaussian tails also can be fitted to that in [1] by using two phenomenological parameters. The effect of the intercommuting probability P was also studied there. It was shown that the non-Gaussian tails diminish as P decreases. However the obtained one-point pdf is symmetric for positive and negative temperature fluctuations, hence did not reproduce the non-zero skewness reported in [1].

In this paper, we study in depth the non-Gaussian features, especially skewness, of the CMB temperature fluctuations due to cosmic (super-)strings, and interpret numerical results obtained in [1]. For this purpose, we adopt a simple model of string network and perform Monte Carlo simulations. We consider the correlation between the curvature and

the velocity of string segments as the origin of skewness and study the dependence of the skewness on the intercommuting probability P .

This paper is organized as follows. In section 2, we give a brief review of the derivation of basic equations for the evolution of string segments incorporating the intercommuting probability P [24]. In section 3 we introduce general formulae for the temperature fluctuations due to cosmic strings [23, 28, 29]. We also discuss the correlation between the curvature and velocity of string segments which gives rise to the skewness in the one point pdf. Then, in section 4, we give the result of our Monte Carlo simulations. We show that the obtained one-point pdf has a negative skewness when the correlations are taken into account. The skewness is plotted as a function of P . Finally, we summarize our results in section 5.

2. An analytic model of the string network

A string worldsheet can be described by $x^\mu = x^\mu(\sigma^a)$, where x^μ and σ^a are the spacetime coordinates and worldsheet coordinates, respectively. The induced metric of the worldsheet γ_{ab} is given by

$$\gamma_{ab} = g_{\mu\nu} \frac{dx^\mu}{d\sigma^a} \frac{dx^\nu}{d\sigma^b}, \quad (2.1)$$

where $g_{\mu\nu}$ is the spacetime metric. We assume that the action for the string dynamics is well approximated by the Nambu-Goto action:

$$S_{\text{NG}} = \mu \int \sqrt{-\gamma} d^2\sigma, \quad (2.2)$$

where μ is the tension of the cosmic string.

Let us consider string dynamics in Friedmann-Lemaître-Robertson-Walker universes with the metric

$$ds_{\text{FLRW}}^2 = a^2(\eta) (-d\eta^2 + d\mathbf{r}^2). \quad (2.3)$$

We choose the temporal gauge :

$$\sigma^0 = \eta, \quad \sigma^1 = \sigma, \quad \dot{\mathbf{r}} \cdot \mathbf{r}' = 0, \quad (2.4)$$

where the bold letters denote the 3-vectors on the comoving space and the dot and the prime denote the derivative with respect to η and σ , respectively. The equations of motion on the cosmological backgrounds are given by [30]

$$\ddot{\mathbf{r}} + 2\mathcal{H} (1 - \dot{\mathbf{r}}^2) \dot{\mathbf{r}} = \frac{1}{\epsilon} \left(\frac{\mathbf{r}'}{\epsilon} \right)', \quad (2.5)$$

$$\dot{\epsilon} = -2\mathcal{H}\epsilon\dot{\mathbf{r}}^2, \quad (2.6)$$

where $\mathcal{H} \equiv \dot{a}/a$ and ϵ is the energy per unit coordinate length defined by

$$\epsilon = \left[\frac{\mathbf{r}'^2}{1 - \dot{\mathbf{r}}^2} \right]^{1/2}. \quad (2.7)$$

We define the total energy E and the average root-mean-square velocity of a string:

$$E = \mu a(\eta) \int \epsilon d\sigma, \quad v_{\text{rms}}^2 = \langle \dot{\mathbf{r}}^2 \rangle \equiv \frac{\int \dot{\mathbf{r}}^2 \epsilon d\sigma}{\int \epsilon d\sigma}. \quad (2.8)$$

In the velocity-dependent one-scale model (VOS), the string network is characterized by only two physical quantities: the correlation length ξ and the rms velocity v_{rms} . The correlation length ξ is defined by

$$\xi \equiv \sqrt{\frac{\mu}{\rho}}, \quad (2.9)$$

where ρ is the total string energy density, which related to E as

$$\rho \propto E/a^3. \quad (2.10)$$

In our treatment, we also take the energy loss due to loop formations into account. A loop formation can occur through the intercommutation of two segments or self-intercommutation of a single segment. The characteristic time scale of the interval of loop formations with the intercommutation probability P is $\sim \xi/(Pv_{\text{rms}})$. Then the energy loss due to the loop formation can be described as

$$\left(\frac{d\rho}{dt} \right)_{\text{to loops}} = -\tilde{c} P v_{\text{rms}} \frac{\rho}{\xi}, \quad (2.11)$$

where we have introduced \tilde{c} as a constant which represents the efficiency of loop formations.

For brevity, we use the quantity $\gamma \equiv 1/H\xi$ rather than ξ with $H = a\mathcal{H}$. For a universe with the scale factor $a(t) \propto t^\beta$ with physical time $t \equiv \int a(\eta) d\eta$, the equations of motion for γ and v_{rms} can be derived from Eqs. (2.8) - (2.11) as [24, 25, 26, 27]

$$\frac{t}{\gamma} \frac{d\gamma}{dt} = 1 - \beta - \frac{1}{2} \beta \tilde{c} P v_{\text{rms}} \gamma - \beta v_{\text{rms}}^2, \quad (2.12)$$

$$\frac{dv_{\text{rms}}}{dt} = (1 - v_{\text{rms}}^2) \left[\frac{k}{R} - 2Hv_{\text{rms}} \right], \quad (2.13)$$

where we have replaced $\langle (\dot{\mathbf{r}}^2)^2 \rangle$ by $\langle \dot{\mathbf{r}}^2 \rangle^2$. The momentum parameter k and the curvature radius R are defined below. For the curvature term, we set

$$\frac{\partial^2 \mathbf{r}}{\partial \hat{s}^2} = \frac{a(\eta)}{R} \hat{\mathbf{u}}, \quad (2.14)$$

where we have introduced the proper coordinate length measure along a string by $d\hat{s} \equiv |\mathbf{r}'| d\sigma = \sqrt{1 - \dot{\mathbf{r}}^2} \epsilon d\sigma$ and $\hat{\mathbf{u}}$ is the unit vector parallel to the curvature radius vector on the comoving space. The momentum parameter k is defined by

$$k \equiv \frac{\langle (1 - \dot{\mathbf{r}}^2)(\dot{\mathbf{r}} \cdot \hat{\mathbf{u}}) \rangle}{v_{\text{rms}}(1 - v_{\text{rms}}^2)} = \frac{R}{a(\eta)v_{\text{rms}}(1 - v_{\text{rms}}^2)} \left\langle \dot{\mathbf{r}} \cdot \frac{1}{\epsilon} \left(\frac{\mathbf{r}'}{\epsilon} \right)' \right\rangle. \quad (2.15)$$

In this paper, we use an approximated form of k [25]:

$$k(v_{\text{rms}}) = \frac{2\sqrt{2}}{\pi} \frac{1 - 8v_{\text{rms}}^6}{1 + 8v_{\text{rms}}^6}. \quad (2.16)$$

It is known that a string network approaches the scaling regime where the characteristic scale grows with the horizon size [31, 32]. For our Monte Carlo simulations, we assume that the scaling is already realized by the time photons leave the last scattering surface. This means that γ and v_{rms} are constant in time. Hence we set the left-hand sides of Eqs. (2.12) and (2.13) equal to zero. We solve them numerically with the assumptions that the universe is in the matter-dominated era, $\beta = 2/3$, and the curvature radius is equal to the correlation length, $R = \xi$.

3. CMB Temperature Fluctuations

3.1 The Hindmarsh-Stebbins-Veeraraghavan formula

A formula for the temperature fluctuation due to a Nambu-Goto string was derived by Stebbins and Veeraraghavan [28, 29] and by Hindmarsh [23]. The Hindmarsh-Stebbins-Veeraraghavan (HSV) formula is given by

$$\Delta(\mathbf{n}, \mathbf{r}_{\text{obs}}, \eta_{\text{obs}}) \equiv \frac{\Delta T}{T} = -2G\mu \int_{\Sigma} d\sigma \frac{(1 + \mathbf{n} \cdot \dot{\mathbf{r}}) [(X\mathbf{n} + \mathbf{X}) \cdot \mathbf{u}]}{(X + \mathbf{n} \cdot \mathbf{X})(X - \dot{\mathbf{r}} \cdot \mathbf{X})} \Big|_{\eta=\eta_{\text{lc}}(\sigma)}, \quad (3.1)$$

where $\mathbf{X}(\sigma) \equiv \mathbf{r}_{\text{obs}} - \mathbf{r}(\sigma, \eta_{\text{lc}}(\sigma))$ is the comoving position of the observer relative to that of the string, $X \equiv |\mathbf{X}|$, \mathbf{u} is defined by

$$\mathbf{u} \equiv \dot{\mathbf{r}} - \left(\frac{\mathbf{n} \cdot \mathbf{r}'}{1 + \mathbf{n} \cdot \dot{\mathbf{r}}} \right) \mathbf{r}', \quad (3.2)$$

and $\eta_{\text{lc}}(\sigma)$ is the conformal time along the intersection of the observer's past light-cone and the string worldsheet,

$$\eta_{\text{obs}} - \eta_{\text{lc}}(\sigma) = X(\sigma). \quad (3.3)$$

It should be stressed that the temperature fluctuation depends on the string distribution on the observer's past light-cone.

The integration range Σ must be appropriately determined. In our calculation, we consider only a segment of a long cosmic string at each scattering. Namely we take Σ as

$$\Sigma : X^{\perp}(\sigma) < \frac{\xi}{a}, \quad (3.4)$$

where

$$\mathbf{X}^{\perp}(\sigma) \equiv \mathbf{X}(\sigma) - (\mathbf{X}(\sigma) \cdot \mathbf{n}) \mathbf{n}. \quad (3.5)$$

This procedure is consistent with the treatment in our previous paper [24].

It is useful to adopt the small angle approximation to understand various effects contained in the HSV formula. In the small-angle approximation, we assume that the angle between the direction of the source $-\mathbf{X}$ and the line-of-sight \mathbf{n} is sufficiently small. This situation is realized when the length of a string segment, which is approximately equal to

the Hubble radius at the epoch of scattering, is much smaller than the distance between the string and the observer. Thus we have

$$\frac{X^\perp(\sigma)}{X(\sigma)} \ll 1, \quad \mathbf{X}(\sigma) \approx -X\mathbf{n} + \mathbf{X}^\perp + \frac{(X^\perp)^2}{2X}\mathbf{n} + \dots \quad (3.6)$$

This approximation is valid as far as a scattering due to a segment at large redshift $z \gg 1$ is considered.

Let us consider the leading order in the small angle approximation,

$$\Delta \approx -4G\mu \int_{\Sigma} d\sigma \frac{\mathbf{X}^\perp \cdot \mathbf{u}}{(X^\perp)^2} \Big|_{\eta=\eta_c(\sigma)}. \quad (3.7)$$

For convenience, we decompose this into two parts as [28]

$$\Delta \approx \Delta^\parallel + \Delta^\perp, \quad (3.8)$$

$$\Delta^\parallel \equiv 4G\mu \int_{\Sigma} d\sigma \alpha_\parallel \frac{\mathbf{X}^\perp \cdot \frac{d\mathbf{X}^\perp}{d\sigma}}{(X^\perp)^2} \Big|_{\eta_c(\sigma)}, \quad (3.9)$$

$$\Delta^\perp \equiv 4G\mu \int_{\Sigma} d\sigma \frac{|\dot{\mathbf{r}}|}{\sqrt{1-\dot{\mathbf{r}}^2}} \alpha_\perp \frac{(\mathbf{n} \times \mathbf{X}^\perp) \cdot \frac{d\mathbf{X}^\perp}{d\sigma}}{(X^\perp)^2} \Big|_{\eta_c(\sigma)}, \quad (3.10)$$

where the coefficients α_\parallel and α_\perp are defined by

$$\alpha_\parallel = \frac{\mathbf{n} \cdot \mathbf{r}'}{|\mathbf{r}'|^2}, \quad \alpha_\perp = \mathbf{n} \cdot \left(\frac{\mathbf{r}'}{|\mathbf{r}'|} \times \frac{\dot{\mathbf{r}}}{|\dot{\mathbf{r}}|} \right). \quad (3.11)$$

Note that $d/d\sigma$ in the above formulae is the derivative along the intersection of the past light-cone with the worldsheet,

$$\frac{d}{d\sigma} \equiv \frac{\partial}{\partial\sigma} + \frac{d\eta_c(\sigma)}{d\sigma} \frac{\partial}{\partial\eta}. \quad (3.12)$$

We may rewrite Eq. (3.9) by integration by part as

$$\Delta^\parallel = -4G\mu \int_{\Sigma} d\sigma \frac{d\alpha_\parallel}{d\sigma} \ln \left(\frac{X^\perp}{L_{\text{cut}}} \right) \Big|_{\eta_c(\sigma)}, \quad (3.13)$$

where L_{cut} is the cutoff scale of the scattering, $L_{\text{cut}} = \xi/a$. It is easy to see from this expression that for an exactly straight and uniformly moving segment, that is for $\dot{\mathbf{r}} = \text{const.}$ and $\mathbf{r}' = \text{const.}$, Δ^\parallel vanishes.

If the segment has a kink at $\sigma = \sigma_k$, we have

$$\alpha_\parallel = \alpha_\parallel^{(+)} \Theta(\sigma - \sigma_k) + \alpha_\parallel^{(-)} \Theta(\sigma_k - \sigma), \quad (3.14)$$

where $\alpha_\parallel^{(\pm)}$ are the constant parameters characterizing the kink and $\Theta(\sigma)$ denotes the Heaviside step function. Then, Δ^\parallel reproduces the kink temperature fluctuation,

$$\Delta^\parallel \approx \Delta_{\text{kink}} = -4G\mu \alpha_{\text{kink}} \ln \frac{X^\perp(\sigma_k)}{L_{\text{kink}}}, \quad (3.15)$$

where we have defined $\alpha_{\text{kink}} = \alpha_{\parallel}^{(+)} - \alpha_{\parallel}^{(-)}$ and L_{kink} is a mean distance between kinks [24, 29, 28]. If the curvature of the segment is taken into account, $d\alpha_{\parallel}/d\sigma \neq 0$ and Δ^{\parallel} appears. Therefore, Δ^{\parallel} can be regarded as contributions of the deficits on the segment (kinks and cusps) and the curvature of the segment.

For an exactly straight and uniformly moving segment, the position of the segments, $\mathbf{X}^{\perp}(\sigma)$, can be written as

$$\mathbf{X}^{\perp}(\sigma) = \boldsymbol{\delta} + \sigma \left| \frac{d\mathbf{X}^{\perp}}{d\sigma} \right| \mathbf{e}, \quad (3.16)$$

where we have introduced the impact parameter $\boldsymbol{\delta} \equiv \mathbf{X}^{\perp}(\sigma = 0)$, $\delta \equiv |\boldsymbol{\delta}|$, and the unit tangent vector $\mathbf{e} \propto d\mathbf{X}^{\perp}/d\sigma$. Then Δ^{\perp} becomes

$$\begin{aligned} \Delta^{\perp} &\approx -4G\mu \frac{|\dot{\mathbf{r}}|}{\sqrt{1-\dot{\mathbf{r}}^2}} \alpha_{\perp} \left[\arctan \left(\frac{|\frac{d\mathbf{X}^{\perp}}{d\sigma}| \sigma + \delta \cos \varphi}{\delta \sin \varphi} \right) \right]_{\sigma_-}^{\sigma_+} \\ &\approx -8G\mu \frac{|\dot{\mathbf{r}}|}{\sqrt{1-\dot{\mathbf{r}}^2}} \alpha_{\perp} \arctan \left(\frac{\xi}{a \delta \sin \varphi} \right), \end{aligned} \quad (3.17)$$

where $\boldsymbol{\delta} \cdot \mathbf{e} \equiv \delta \cos \varphi$. It is clear to see that the dominant contributions are given from the string portions with $|\sigma| \lesssim \delta / |\frac{d\mathbf{X}^{\perp}}{d\sigma}|$. This is just the Gott-Kaiser-Stebbins (GKS) effect [16, 17]. Hence Δ^{\perp} may be regarded as the generalization of the GKS effect. If the curvature of the segment is taken into account, correction terms due to higher derivatives will appear in Δ^{\perp} .

Although most scatterings occur at $z \gg 1$, some photons may be scattered by a segment at $z \sim \mathcal{O}(1)$. Therefore it is desirable to check the validity of the small angle approximation. For this purpose, in our Monte Carlo simulations, we have taken into account the next order corrections and compared the result with the one obtained in the leading order approximation. We found no difference between these two, supporting the validity of the small angle approximation.

3.2 The Gott-Kaiser-Stebbins effect

Next we consider the GKS effect [16, 17]. Using Eq. (3.17), the rms temperature fluctuation due to the GKS effect of a string is estimated as

$$\Delta_{\text{GKS}} = 8 \frac{v_{\text{rms}}}{\sqrt{1-v_{\text{rms}}^2}} \alpha_{\text{seg}} G\mu \arctan \left(\frac{\xi}{a\delta} \right). \quad (3.18)$$

where $\alpha_{\text{seg}} = \langle \alpha_{\perp}^2 \rangle^{1/2}$. In the case of a close encounter, i.e. $\delta \ll \xi/a$, this reduces to

$$\Delta_{\text{GKS}} \approx 4\pi \frac{v_{\text{rms}}}{\sqrt{1-v_{\text{rms}}^2}} \alpha_{\text{seg}} G\mu, \quad (3.19)$$

Thus, this produces the discontinuity of the temperature fluctuations across the moving string segment when photons passes by the moving string.

The temperature fluctuation due to a segment approaches zero when the impact parameter is larger than the segment length ξ . This implies that a segment has an effective

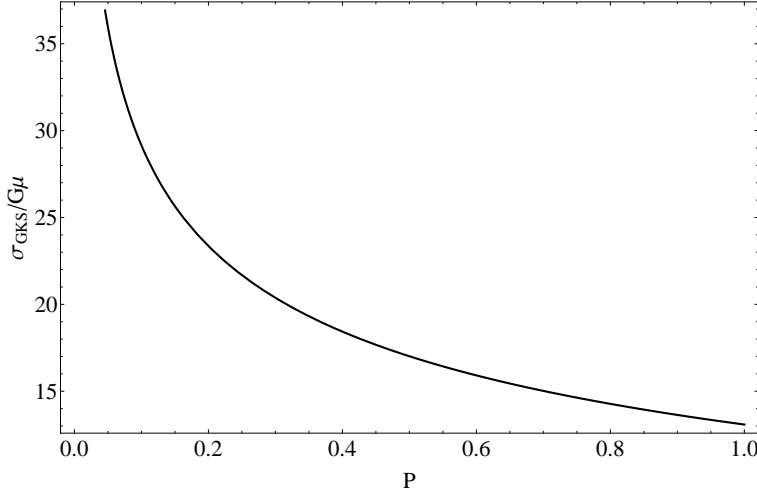


Figure 1: The standard deviation of the Gaussian components of the pdf due to GKS effects, σ_{GKS} as a function of intercommuting probability P .

cross section $\sim \xi^2$. In terms of ξ , the number of segments in a horizon volume is expressed as $N_{\text{seg}} = 1/\xi^3 H^3 = \gamma^3$. Therefore the optical depth for a CMB photon is

$$\begin{aligned} \tau_{\text{opt}} &= \int_0^{z_{\text{LSS}}} N_{\text{seg}} H^3 \xi^2 \frac{dz}{H(1+z)} = \gamma \log(1 + z_{\text{LSS}}) \\ &\approx 16 \left(\frac{\tilde{c}P}{0.23} \right)^{-1/2}, \end{aligned} \quad (3.20)$$

where $\gamma \approx (3\tilde{c}P/\sqrt{2\pi^2})^{-1/2}$, and we have put $z_{\text{LSS}} \approx 1100$ and used $\tilde{c} \approx 0.23$ as the standard value [33]. Since $\tau_{\text{opt}} \gg 1$, a photon ray is scattered by segments many times on its way from the last scattering surface to the observer. Therefore, the temperature fluctuations behave like a random walk and the one-point pdf becomes well approximated by a Gaussian distribution as a result of the central limit theorem. Thus the GKS effect gives the Gaussian component of the one-point pdf,

$$\frac{dP}{d\Delta_{\text{GKS}}} \approx \frac{1}{\sqrt{2\pi}\sigma_{\text{GKS}}} e^{-\Delta^2/2\sigma_{\text{GKS}}^2}, \quad (3.21)$$

where the standard deviation is estimated as

$$\sigma_{\text{GKS}} = \Delta_{\text{GKS}} \frac{\sqrt{\tau_{\text{opt}}}}{2} \approx 13G\mu \left(\frac{\alpha_{\text{seg}}}{1/\sqrt{2}} \right) \left(\frac{\tilde{c}P}{0.23} \right)^{-1/4}, \quad (3.22)$$

which is shown in Fig. 1 as a function of intercommuting probability P . In [24], we found that the above estimate of the standard deviation agrees well with the result of numerical simulations (for $P = 1$) by Fraisse et al. [1].

3.3 Correlations as sources of the skewness

The one-point pdf of the temperature fluctuations due to the GKS effect is symmetric under $\Delta \rightarrow -\Delta$ since the form of the GKS effect is obviously symmetric as is seen from Eq. (3.18).

However, a skewness may appear if we take account of the curvature of segments and its correlations with the velocity, as discussed in [24, 20]. If a segment has a curvature, the probability of producing positive or negative temperature deviation becomes asymmetric. The amplitude of the asymmetry depends on the angle between the curvature vector and the velocity vector of the segment. However, if the curvature and the velocity are not correlated, the statistical averaging results in a vanishing skewness. Therefore, a correlation between the velocity vector and the curvature vector is necessary to produce a skewness. In this paper, we investigate two kinds of correlation. One is due to the breaking of the time reversal symmetry caused by the cosmic expansion, which has been already pointed out in [20]. The other is due to the effective curvature of a string on its intersection with the observer's past light-cone. We call this "light-cone effect".

3.3.1 Correlation due to cosmic expansion

From Eq. (2.13), assuming the scaling regime, we have

$$\frac{k}{R} = \frac{1}{av_{\text{rms}}(1 - v_{\text{rms}}^2)} \left\langle \dot{\mathbf{r}} \cdot \frac{1}{\epsilon} \left(\frac{\mathbf{r}'}{\epsilon} \right)' \right\rangle \approx 2Hv_{\text{rms}}. \quad (3.23)$$

It is easy to see that a nontrivial correlation between the velocity vector $\dot{\mathbf{r}}$ and the curvature vector \mathbf{r}'' exists if there is Hubble expansion. Each configuration of string segments must be consistent with this correlation. We use this expression when we perform our Monte Carlo simulation. A method for determining string segment configurations in our simulations is explained in section 4.

3.3.2 Light-cone effect

In the HSV formula, Eq. (3.1), the integration is along the light-cone. In the small angle approximation, the coordinates of a string on the past light-cone emanating from the observer, $\mathbf{X}(\sigma)$, can be expanded as

$$\begin{aligned} \mathbf{X}(\sigma) &= \mathbf{X}_0 + \left(\frac{d\mathbf{X}}{d\sigma} \right)_0 \sigma + \frac{1}{2} \left(\frac{d^2\mathbf{X}}{d\sigma^2} \right)_0 \sigma^2 + \mathcal{O}(\sigma^3) \\ &= \mathbf{X}_0 - \left[\mathbf{r}'_0 + \left(\frac{d\eta_{\text{lc}}}{d\sigma} \right)_0 \dot{\mathbf{r}}_0 \right] \sigma \\ &\quad - \frac{1}{2} \left[\mathbf{r}''_0 + \left(\frac{d\eta_{\text{lc}}}{d\sigma} \right)_0^2 \ddot{\mathbf{r}}_0 + 2 \left(\frac{d\eta_{\text{lc}}}{d\sigma} \right)_0 \dot{\mathbf{r}}'_0 + \left(\frac{d^2\eta_{\text{lc}}}{d\sigma^2} \right)_0 \dot{\mathbf{r}}_0 \right] \sigma^2 + \mathcal{O}(\sigma^3), \end{aligned} \quad (3.24)$$

where $d\eta_{\text{lc}}/d\sigma$ and $d^2\eta_{\text{lc}}/d\sigma^2$ are estimated from Eqs. (3.3) and (3.6) as

$$\left(\frac{d\eta_{\text{lc}}}{d\sigma} \right)_0 = -\frac{\mathbf{n} \cdot \mathbf{r}'_0}{1 + \mathbf{n} \cdot \dot{\mathbf{r}}_0}, \quad (3.25)$$

$$\begin{aligned} \left(\frac{d^2\eta_{\text{lc}}}{d\sigma^2} \right)_0 &= -\frac{1}{1 + \mathbf{n} \cdot \dot{\mathbf{r}}_0} \left[\frac{1 - \dot{\mathbf{r}}_0^2}{X_0} \left\{ \frac{\mathbf{r}'_0{}^2}{1 - \dot{\mathbf{r}}_0^2} - \left(\frac{d\eta_{\text{lc}}}{d\sigma} \right)_0^2 \right\} \right. \\ &\quad \left. + \mathbf{n} \cdot \left\{ \mathbf{r}''_0 + \left(\frac{d\eta_{\text{lc}}}{d\sigma} \right)_0^2 \ddot{\mathbf{r}}_0 + 2 \left(\frac{d\eta_{\text{lc}}}{d\sigma} \right)_0 \dot{\mathbf{r}}'_0 \right\} \right]. \end{aligned} \quad (3.26)$$

It is remarkable that even if a string is exactly straight and moves uniformly, $\mathbf{r}_0'' = \dot{\mathbf{r}}_0 = \dot{\mathbf{r}}_0' = 0$, it always has an “effective curvature”. Namely,

$$\left(\frac{d^2\mathbf{r}}{d\sigma^2}\right)_0 = \left(\frac{d^2\eta_{\text{lc}}}{d\sigma^2}\right)_0 \dot{\mathbf{r}}_0 \neq \mathbf{0}, \quad (3.27)$$

where note that $d/d\sigma$ is a derivative along the light-cone; see Eq. (3.12). This obviously means the existence of a correlation between the effective curvature and the velocity of the segment. However, this effect is subdominant in the small angle approximation, because of the suppression factor σ/X_0 in Eq. (3.24), where X_0 is of the order of the angular diameter distance from the string to the observer. Thus as far as scatterings at $z > 1$ are concerned, the light-cone effect is smaller than the effect due to cosmic expansion.

4. Monte Carlo simulations for the one-point pdf

4.1 Setup

We compute the one-point pdf of the small-angle CMB temperature fluctuations due to curved string segments with a simple model of the string network (VOS) by performing Monte Carlo simulations.

4.1.1 Scattering probability

Curved segments are assumed to be located randomly between the LSS and the present time consistently with the VOS model. We divide the redshift range $0 < z < z_{\text{LSS}}$ into a number of bins with the width

$$\Delta \log(1+z) = \frac{\log(1+z_{\text{LSS}})}{\tau_{\text{opt}}} \Delta p = \frac{\Delta p}{\gamma}, \quad (4.1)$$

where Δp is the scattering probability assigned to each bin. The scattering events due to cosmic strings can be randomly arranged on the observer’s line-of-sight by using Eq. (4.1). We set $\Delta p = 10^{-2}$ in our simulations.

4.1.2 Assumptions and the expansion of the HSV formula

To take into account the curvature of a string segment, we expand $\mathbf{X}^\perp(\sigma)$ to second order in σ as given by (3.24). We assume the higher order terms are negligible. Hence we set

$$\frac{\mathbf{X}^\perp(\sigma)}{X_0} = \frac{\boldsymbol{\delta}}{X_0} + \left(\frac{d\mathbf{X}^\perp}{d\sigma}\right)_0 \frac{\sigma}{X_0} + \frac{1}{2} \left(\frac{d^2\mathbf{X}^\perp}{d\sigma^2}\right)_0 \frac{\sigma^2}{X_0}. \quad (4.2)$$

We also assume the validity of the small angle approximation and assume $\delta/X_0 = O(\varepsilon)$ and $|\frac{d\mathbf{X}^\perp}{d\sigma}|_0 \sigma/X_0 = O(\varepsilon)$, where ε is a small expansion parameter. Furthermore, we assume that the curvature \mathbf{r}_0'' , the rotation $\dot{\mathbf{r}}_0'$ and the acceleration $\ddot{\mathbf{r}}_0$ of a string segment can be treated as perturbations from a uniformly moving straight string segment,

$$|\mathbf{r}_0''|\sigma \sim |\ddot{\mathbf{r}}_0|\sigma \sim |\dot{\mathbf{r}}_0'|\sigma = \mathcal{O}(\varepsilon) \ll 1. \quad (4.3)$$

The above order estimate comes from the fact that $\mathbf{r}''\sigma \sim \sigma/\xi \sim \sigma/X_0$. Note that these order estimates imply that the first two, leading order terms in (4.2) are already of $O(\varepsilon)$ and hence the last curvature term, which is $O(\varepsilon^2)$, is only $O(\varepsilon)$ relative to the leading order terms.

Now we can expand the reduced HSV formula Eq. (3.7). As discussed in the above, the effect of the curvature appears $O(\varepsilon)$ relative to the leading order terms. Therefore, we expand the numerator $\mathbf{X}^\perp \cdot \mathbf{u}$ to $O(\sigma^2)$ and the denominator $(X^\perp)^2$ to $O(\sigma^3)$. Hence it can be written as

$$\Delta \approx -4G\mu \int_{\Sigma} d\sigma \frac{\sum_{i=0}^2 \alpha_i \sigma^i}{\sum_{j=0}^3 \beta_j \sigma^j}, \quad (4.4)$$

where α_i ($i = 0, 1, 2$) and β_j ($j = 0, 1, 2, 3$) are given in Appendix A. Once the string configuration is fixed at each scattering event, we can immediately calculate the temperature deviation using Eq.(4.4).

4.1.3 Degrees of freedom of a string configuration

Our remaining task is to determine string configurations. A string configuration can be characterized by several random variables. Details about the random variables are discussed in Appendix B. Here, we just count the number of degrees of freedom (dofs) to determine a string configuration.

For a string segment with the curvature taken into account, originally we have 3 dof for \mathbf{r}_0 , 6 dof for $\dot{\mathbf{r}}_0$ and \mathbf{r}'_0 , and 9 dof for $\ddot{\mathbf{r}}_0$, $\dot{\mathbf{r}}'_0$ and \mathbf{r}''_0 . For \mathbf{r}_0 , using the coordinate dof, there remains only 1 dof, which is the impact parameter δ . For $\dot{\mathbf{r}}_0$ and \mathbf{r}'_0 , the number of dof is reduced to 4 by using 2 constraint equations (the gauge condition and the normalization) for the string dynamics. The remaining dof are the magnitude of the velocity v and the 3 angular parameters (θ, ϕ, ψ) that determine the direction along the string and the velocity vector in the plane orthogonal to the string direction. Finally, the number of dof of $\ddot{\mathbf{r}}_0$, $\dot{\mathbf{r}}'_0$ and \mathbf{r}''_0 is reduced to 4 using 3 equations of motion and 2 constraints. One of them corresponds to the inner product of the velocity vector and the curvature vector, $\dot{\mathbf{r}}_0 \cdot \mathbf{r}''_0$. The remaining 3 dof correspond to the curvature vector orthogonal to $\dot{\mathbf{r}}_0$ and the rotation of the string segment orthogonal to both $\dot{\mathbf{r}}_0$ and \mathbf{r}''_0 . Lacking the knowledge of how much freely moving string segments would be curved, we set these remaining 3 dof to zero for simplicity. Thus we have 6 dof in total, $(\delta, v, \theta, \phi, \psi, \dot{\mathbf{r}}_0 \cdot \mathbf{r}''_0)$.

In this paper, we further reduce the dof by fixing the velocity and using the scaling assumption. First we set $v = v_{\text{rms}}$. In the scaling regime, the curvature of a string segment and the velocity must be correlated. Locally at each event of scattering, one may neglect the Hubble expansion, and we have

$$\frac{1}{a} \left\langle \dot{\mathbf{r}} \cdot \frac{1}{\epsilon} \left(\frac{\mathbf{r}'}{\epsilon} \right)' \right\rangle \approx \left\langle \frac{\dot{\mathbf{r}} \cdot \mathbf{r}''}{a} \right\rangle \approx \frac{\dot{\mathbf{r}}_0 \cdot \mathbf{r}''_0}{a} \approx 2Hv_{\text{rms}}^2 (1 - v_{\text{rms}}^2). \quad (4.5)$$

Then

$$\dot{\mathbf{r}}_0 \cdot \mathbf{r}''_0 = 2aHv_{\text{rms}}^2 (1 - v_{\text{rms}}^2). \quad (4.6)$$

Thus, the remaining dof are $(\delta, \theta, \phi, \psi)$. For a demonstration of the temperature fluctuation due to a curved segment, we show the CMB map with $\theta = \phi = \pi/2$ and $\psi = 0$ in Fig. 3.

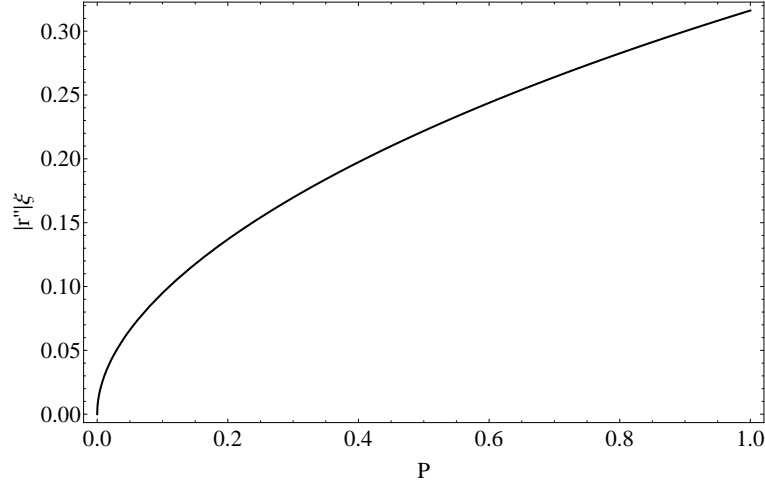


Figure 2: The amplitude of the curvature vector normalized by $\xi = 1/H\gamma$, $|\mathbf{r}''|\xi = (\mathbf{r}_0'' \cdot \dot{\mathbf{r}}_0 / v_{\text{rms}})\xi = \mathcal{O}(\varepsilon)$ as a function of P .

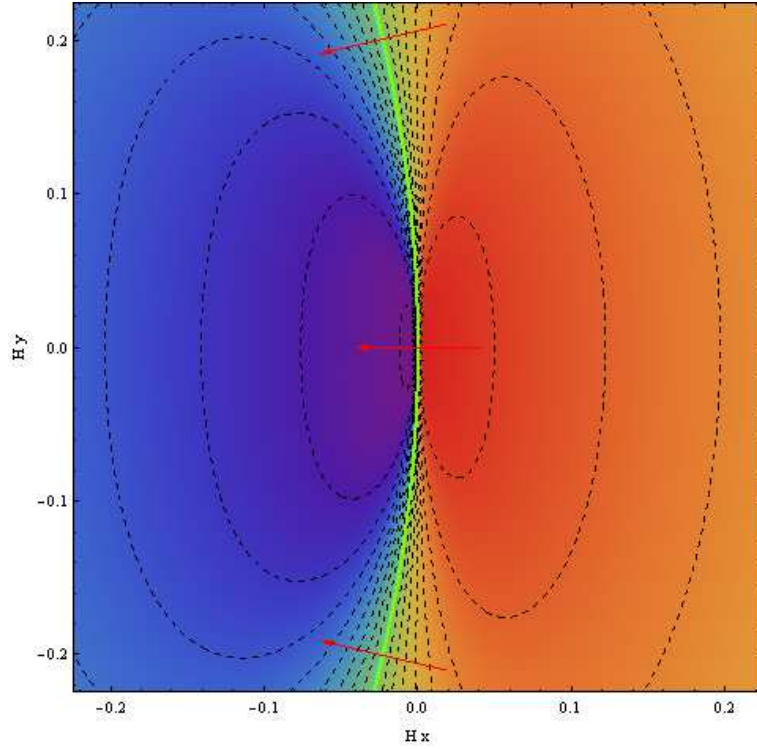


Figure 3: The map of the temperature fluctuations due to a curved string segment with $\theta = \phi = \pi/2$ and $\psi = 0$. Also we define (Hx, Hy) as the Hubble normalized two-dimensional coordinate relative to $\sigma = 0$ in the small patch of sky. The green line denotes the position of the string segment, $\mathbf{X}^\perp(\sigma)$, the dashed lines are contour lines with the width $1G\mu$ and the red vectors are the velocity vectors at each point.

4.2 Numerical Results

We performed Monte Carlo simulations with 10^7 photons on NEC Express 5800 XeonMP

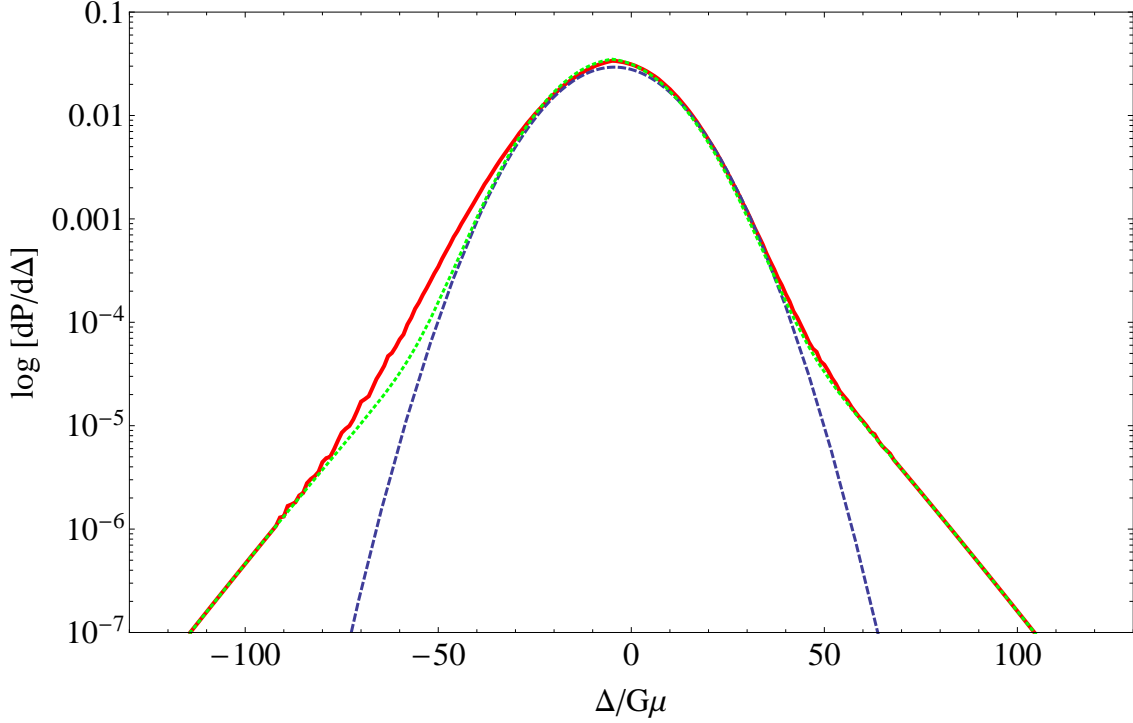


Figure 4: The one-point pdf of the CMB temperature fluctuations induced by curved cosmic strings and kinks for the intercommuting probability $P = 1$. The solid curve (in red) is the one-point pdf obtained by averaging over scattering of 10^7 photons by curved string segments, added on top of an analytic pdf for kinks obtained in [24]. The dashed line (in blue) is the best Gaussian fit. The dotted line (in green) represents the one-point pdf for straight segments and kinks.

3.16GHz at Yukawa Institute for Theoretical Physics, Kyoto University. It took two CPU days for $P = 1$, three CPU days for $P = 0.5$ and five CPU days for $P = 0.1$.

For $P = 1$, the obtained one-point pdf of the total temperature fluctuations is shown in Fig. 4. In order to take into account the contribution from kinks, we just added an analytic pdf for kinks obtained in our previous paper (3.15). The one-point pdf significantly deviates from the best Gaussian fit. The sample standard deviation is $\sigma_{\text{sim}}(P = 1) \approx 14G\mu$, consistent with the analytical estimate in [24] and Fig. 1 as well as with the numerical result of [1]. The sample skewness measured in Fig. 4 is

$$g_1(P = 1) = \frac{\overline{(\Delta - \bar{\Delta})^3}}{\sigma_{\Delta}^3} \approx -0.14. \quad (4.7)$$

Thus the one-point pdf has a negative skewness.

In order to investigate the dependence of the one-point pdf on the intercommuting probability P , we computed the one-point pdfs for $P = 0.5$ and $P = 0.1$ and the obtained one-point pdfs are shown in Figs. 5 and 6. The standard deviations are $\sigma_{\text{sim}}(P = 0.5) \approx 18G\mu$ for $P = 0.5$ and $\sigma_{\text{sim}}(P = 0.1) \approx 31G\mu$ for $P = 0.1$. These are consistent with the

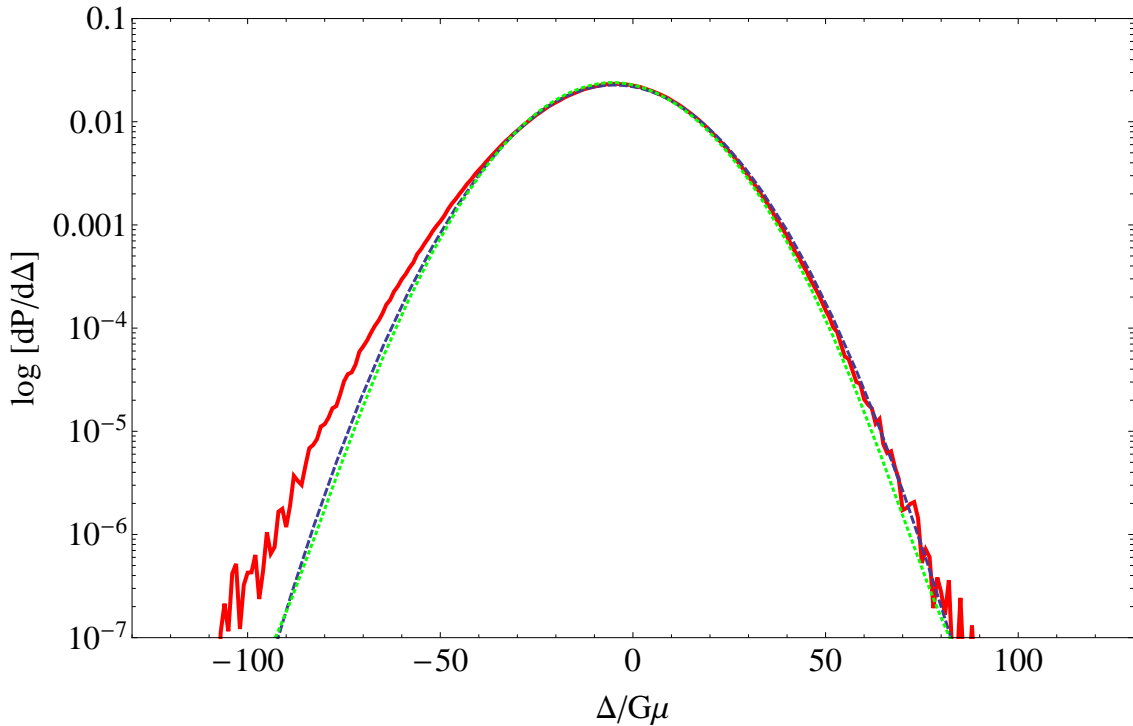


Figure 5: The same as Fig. 4 but for the intercommuting probability $P = 0.5$.

analytical estimate in [24] and Fig. 1. The sample skewness was found as

$$g_1(P < 1) = \begin{cases} -0.11 & \text{for } P = 0.5, \\ -0.04 & \text{for } P = 0.1. \end{cases} \quad (4.8)$$

Furthermore, we calculated the skewness for various values of P and obtained a power-series best fit in Fig. 7. As we see, the dispersion of the Gaussian part increases as P decreases (see Fig. 1) and the non-Gaussian features, i.e., the skewness and the non-Gaussian tail, are suppressed. Our result suggests that the sample skewness for a sufficiently small P approaches $g_1 \lesssim (\text{a few}) \times 10^{-2}$.

5. Summary

In this paper, we have computed the one-point pdf of small-angle CMB temperature fluctuations due to the “curved” cosmic (super-)string segments by performing Monte Carlo simulations. Our purpose was to examine the numerical result obtained in [1] with a simple model of the string network under a few reasonable assumptions, i.e., the velocity-dependent one-scale (VOS) model. We have found that the presence of the nonzero momentum parameter k corresponds to the correlation between the curvature and the velocity of segments, and therefore the Hubble expansion is essential for a nontrivial correlation (see Eq. (2.15) and Eq. (3.23)). We have also found another type of correlation between the curvature and the velocity induced by the effective curvature along the intersection of a

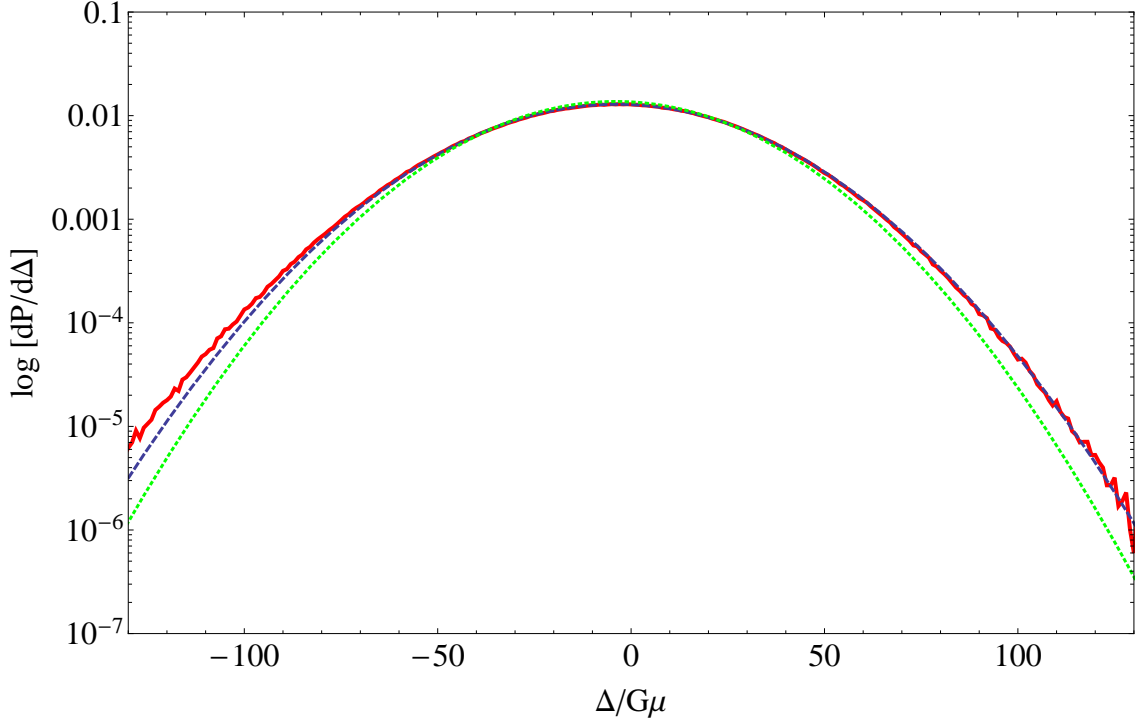


Figure 6: The same as Fig. 4 but for the intercommuting probability $P = 0.1$.

string worldsheet and the observer’s past light-cone (“light-cone effect”). The light-cone effect always exists independent from the properties of string configuration and the cosmic volume expansion.

Combining these two effects, we have calculated the one-point pdf numerically and showed that it reproduces features of the numerical simulations in [1] very well. In particular, we have found that the one-point pdf has a negative skewness. It was also found that as P decreases the standard deviation of the Gaussian part increases and the non-Gaussian tails and the skewness are suppressed. Our result suggests that, for the sufficiently small P , the skewness approaches $\lesssim (\text{a few}) \times 10^{-2}$.

Note that the observed temperature fluctuations are given by contributions not only from cosmic (super-)strings but also from primary and other secondary anisotropies. It is known that conventional cosmic strings can contribute at most 10% of the total power at $\ell = 10$ in the CMB fluctuations [11]. Thus, in real world, contributions from primary anisotropies make the skewness significantly small on large angular scales. In order to suppress this effect of the large-scale anisotropies, it would be effective to choose an observation area of a sufficiently small angular size ($\sim O(10)\text{arcmin}^2$) where the primary CMB fluctuations have been completely damped out. This would remove the contribution of the primary fluctuations to the denominator of the skewness formula (see Eq. (1.1)), hence enhance the observability of the skewness.

It is known that $O(0.1)$ skewness would indicate nonlinear parameter $|f_{\text{NL}}| \approx O(10^3)$ [34, 20]. In this paper, we have shown that, for smaller intercommuting probability P , non-

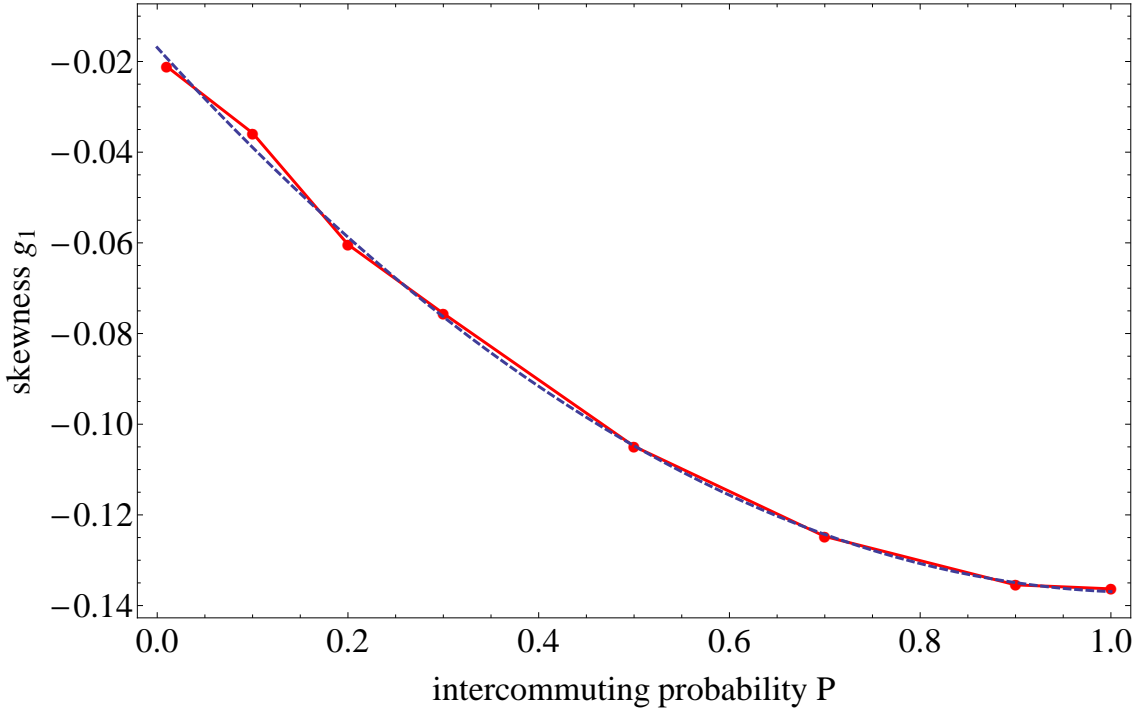


Figure 7: The skewness as a function of the intercommuting probability P . The solid dots (in red) are the skewness obtained by simulations, each with 10^7 photons. The dashed line (in blue) is the power-series best fit function: $g_1(P) \approx 0.11P^2 - 0.23P - 0.02$.

Gaussian features become more difficult to find. To discuss the relation between the skewness and the non-Gaussian parameter f_{NL} in the bispectrum, it is important to compute the angular power spectrum in our model. The work along this direction is in progress [35]. Since the non-Gaussian features significantly depend on the intercommuting probability, they could help us to distinguish field theoretic cosmic strings and cosmic superstrings.

Acknowledgments

DY thanks T. Azeyanagi, T.W.B. Kibble, K. Murata, A. Linde, Y. Sekino, T. Tanaka and V. Vanchurin for useful comments. We thank the organizers and participants of “The non-Gaussian Universe” workshop at Yukawa Institute for Theoretical Physics for stimulating discussion and presentations. Numerical computation in this work was carried out on NEC 3.16 GHz at Yukawa Institute for Theoretical Physics. This work was supported in part by Monbukagakaku-sho Grant-in-Aid for the Global COE programs “The Next Generation of Physics, Spun from Universality and Emergence” at Kyoto University and “Quest for Fundamental Principles in the Universe: from Particles to the Solar System and the Cosmos” at Nagoya University. This work was also supported by JSPS Grant-in-Aid for Scientific Research (A) No. 18204024 and by Grant-in-Aid for Creative Scientific Research No. 19GS0219. KT was supported by Grand-in-Aid for Scientific Research No. 21840028. YS, DY and AN were supported by Grant-in-Aid for JSPS Fellows No. 19-7852, No. 20-1117 and No. 21-1899 respectively.

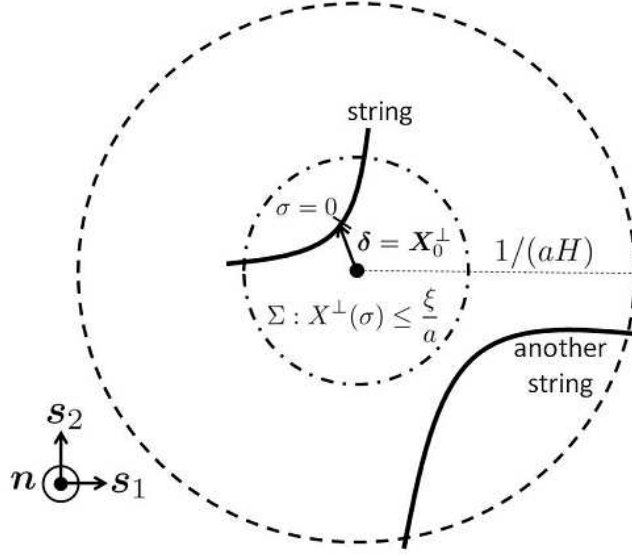


Figure 8: A schematic picture of the surface perpendicular to the line of sight \mathbf{n} at scattering.

A. Reduction of the HSV formula

The reduced HSV formula is

$$\Delta = -4G\mu \int_{\Sigma} d\sigma \frac{\left[\mathbf{X}^{\perp} + \frac{(X^{\perp})^2}{2X} \mathbf{n} \right] \cdot \tilde{\mathbf{u}}}{\left(1 - \frac{\mathbf{X}}{X} \cdot \dot{\mathbf{r}} \right) (X^{\perp})^2} \Big|_{\eta=\eta_c(\sigma)}, \quad (\text{A.1})$$

where we have introduced $\tilde{\mathbf{u}} = (1 + \mathbf{n} \cdot \dot{\mathbf{r}})\mathbf{u}$, and added terms second order in the small angle approximation.

We set

$$\mathbf{X}^{\perp}(\sigma) = \boldsymbol{\delta} + \left(\frac{d\mathbf{X}^{\perp}}{d\sigma} \right)_0 \sigma + \frac{1}{2} \left(\frac{d^2\mathbf{X}^{\perp}}{d\sigma^2} \right)_0 \sigma^2 + O(\varepsilon^3 X_0), \quad (\text{A.2})$$

where we have introduced the expansion parameter ε such that $\delta/X_0 = O(\varepsilon)$, etc., as discussed in 4.1.2. The absolute value of \mathbf{X}^{\perp} is then expanded as

$$\begin{aligned} [X^{\perp}(\sigma)]^2 &= \delta^2 + 2 \left[\boldsymbol{\delta} \cdot \left(\frac{d\mathbf{X}^{\perp}}{d\sigma} \right)_0 \right] \sigma + \left[\left| \frac{d\mathbf{X}^{\perp}}{d\sigma} \right|_0^2 + \boldsymbol{\delta} \cdot \left(\frac{d^2\mathbf{X}^{\perp}}{d\sigma^2} \right)_0 \right] \sigma^2 \\ &\quad + \left[\left(\frac{d\mathbf{X}^{\perp}}{d\sigma} \right)_0 \cdot \left(\frac{d^2\mathbf{X}^{\perp}}{d\sigma^2} \right)_0 \right] \sigma^3 + O(\varepsilon^4 X_0^2) \\ &\equiv a_0 + a_1 \sigma + a_2 \sigma^2 + a_3 \sigma^3 + O(\varepsilon^4 X_0^2). \end{aligned} \quad (\text{A.3})$$

We also have another useful expression,

$$1 - \frac{\mathbf{X}}{X} \cdot \dot{\mathbf{r}} \approx 1 + \mathbf{n} \cdot \dot{\mathbf{r}} - \frac{\mathbf{X}^{\perp} \cdot \dot{\mathbf{r}}}{X} \equiv L_0 + L_1 \sigma + O(\varepsilon^2), \quad (\text{A.4})$$

where

$$L_0 = 1 + \mathbf{n} \cdot \dot{\mathbf{r}}_0 - \frac{\boldsymbol{\delta} \cdot \dot{\mathbf{r}}_0}{X_0}, \quad (\text{A.5})$$

$$L_1 = \left(\mathbf{n} \cdot \frac{d\dot{\mathbf{r}}}{d\sigma} \right)_0 - \frac{1}{X_0} \left[\left(\frac{d\mathbf{X}^\perp}{d\sigma} \right)_0 \cdot \dot{\mathbf{r}}_0 \right]. \quad (\text{A.6})$$

Then the HSV formula due to a curved segment can be approximated as

$$\Delta = -4G\mu \int_\Sigma d\sigma \frac{\sum_{i=0}^2 \alpha_i \sigma^i}{\sum_{j=0}^3 \beta_j \sigma^j}, \quad (\text{A.7})$$

where the coefficients of the numerator are

$$\alpha_0 = \boldsymbol{\delta} \cdot \tilde{\mathbf{u}}_0 + \frac{\delta^2}{2X_0} (\mathbf{n} \cdot \mathbf{u}_0), \quad (\text{A.8})$$

$$\alpha_1 = \boldsymbol{\delta} \cdot \left(\frac{d\tilde{\mathbf{u}}}{d\sigma} \right)_0 + \left(\frac{d\mathbf{X}^\perp}{d\sigma} \right)_0 \cdot \tilde{\mathbf{u}}_0 + \frac{1}{2X_0} \left\{ a_1 (\mathbf{n} \cdot \tilde{\mathbf{u}}_0) + a_0 \left[\mathbf{n} \cdot \left(\frac{d\tilde{\mathbf{u}}}{d\sigma} \right)_0 \right] \right\}, \quad (\text{A.9})$$

$$\alpha_2 = \left(\frac{d\mathbf{X}^\perp}{d\sigma} \right)_0 \cdot \left(\frac{d\tilde{\mathbf{u}}}{d\sigma} \right)_0 + \frac{1}{2} \left[\left(\frac{d^2 \mathbf{X}^\perp}{d\sigma^2} \right)_0 \cdot \tilde{\mathbf{u}}_0 \right], \quad (\text{A.10})$$

and those of the denominator are

$$\beta_0 = L_0 a_0, \quad (\text{A.11})$$

$$\beta_1 = L_0 a_1 + L_1 a_0, \quad (\text{A.12})$$

$$\beta_2 = L_0 a_2 + L_1 a_1, \quad (\text{A.13})$$

$$\beta_3 = L_0 a_3 + L_1 a_2. \quad (\text{A.14})$$

A schematic picture of the relation between the normalized bases and the origin of the worldsheet coordinates is given in Fig. 8.

B. Random Variables

For our Monte Carlo simulations, we need to specify random variables in a physically reasonable way. In our situation, the random variables are those which specify the string configuration at each scattering event. They are the string position \mathbf{r}_0 , the velocity $\dot{\mathbf{r}}_0$, the direction \mathbf{r}'_0 , the curvature \mathbf{r}''_0 , the rotation $\dot{\mathbf{r}}'_0$ and the acceleration \mathbf{r}''_0 . Thus there are 18 parameters in total. However, not all of them are independent from each other because of the equations of motion and constraint equations.

Since at each scattering event, the cosmic expansion can be neglected, the equations of motion can be approximated by those on the Minkowski background. In the conformal and temporal gauge, the equations of motion are given by

$$\ddot{\mathbf{r}} - \mathbf{r}'' = 0. \quad (\text{B.1})$$

The gauge conditions lead constraint equations as

$$\dot{\mathbf{r}} \cdot \mathbf{r}' = 0, \quad \dot{\mathbf{r}}^2 + \mathbf{r}'^2 = 1. \quad (\text{B.2})$$

Differentiating the constraint equations, we have

$$\mathbf{r}_0'' \cdot \dot{\mathbf{r}}_0 = -\mathbf{r}_0' \cdot \dot{\mathbf{r}}_0', \quad \ddot{\mathbf{r}}_0 \cdot \mathbf{r}_0' = -\dot{\mathbf{r}}_0 \cdot \dot{\mathbf{r}}_0'. \quad (\text{B.3})$$

Using Eqs. (B.1)-(B.3), we can derive the following expressions:

$$\mathbf{r}_0' = \sqrt{1-v^2} \mathbf{n}_\parallel, \quad \dot{\mathbf{r}}_0 = v \mathbf{t}_1, \quad (\text{B.4})$$

$$\ddot{\mathbf{r}}_0 = \mathbf{r}_0'' \approx -\frac{v}{\sqrt{1-v^2}} (\dot{\mathbf{r}}_0' \cdot \mathbf{t}_1) \mathbf{n}_\parallel + (\mathbf{r}_0'' \cdot \mathbf{t}_1) \mathbf{t}_1 + (\mathbf{r}_0'' \cdot \mathbf{t}_2) \mathbf{t}_2, \quad (\text{B.5})$$

$$\dot{\mathbf{r}}_0' \approx -\frac{v}{\sqrt{1-v^2}} (\mathbf{r}_0'' \cdot \mathbf{t}_1) \mathbf{n}_\parallel + (\dot{\mathbf{r}}_0' \cdot \mathbf{t}_1) \mathbf{t}_1 + (\dot{\mathbf{r}}_0' \cdot \mathbf{t}_2) \mathbf{t}_2, \quad (\text{B.6})$$

where $(\mathbf{n}_\parallel, \mathbf{t}_1, \mathbf{t}_2)$ are unit basis vectors with \mathbf{n}_\parallel parallel to \mathbf{r}_0' and \mathbf{t}_1 parallel to $\dot{\mathbf{r}}_0$. In terms of coordinate basis vectors $(\mathbf{n}, \mathbf{s}_1, \mathbf{s}_2)$ with \mathbf{n} being the unit vector along the light of sight, those parameters can be written as

$$v = |\dot{\mathbf{r}}_0|, \quad (\text{B.7})$$

$$\mathbf{n}_\parallel = \sin \theta \cos \phi \mathbf{s}_1 + \sin \theta \sin \phi \mathbf{s}_2 + \cos \theta \mathbf{n}, \quad (\text{B.8})$$

$$\begin{aligned} \mathbf{t}_1 = & (-\sin \psi \cos \theta \cos \phi - \cos \psi \sin \phi) \mathbf{s}_1 \\ & + (-\sin \psi \cos \theta \sin \phi + \cos \psi \cos \phi) \mathbf{s}_2 + \sin \psi \sin \theta \mathbf{n}, \end{aligned} \quad (\text{B.9})$$

$$\begin{aligned} \mathbf{t}_2 = & (-\cos \psi \cos \theta \cos \phi + \sin \psi \sin \phi) \mathbf{s}_1 \\ & + (-\cos \psi \cos \theta \sin \phi - \sin \psi \cos \phi) \mathbf{s}_2 + \cos \psi \sin \theta \mathbf{n}, \end{aligned} \quad (\text{B.10})$$

where the ranges of the angular coordinates are

$$0 \leq \theta \leq \pi, \quad 0 \leq \phi \leq 2\pi, \quad 0 \leq \psi \leq 2\pi. \quad (\text{B.11})$$

Thus the total number of degrees of freedom (dof) is reduced to 9; $(\delta, v, (\dot{\mathbf{r}}_0' \cdot \mathbf{t}_1), (\mathbf{r}_0'' \cdot \mathbf{t}_1), (\dot{\mathbf{r}}_0' \cdot \mathbf{t}_2), (\mathbf{r}_0'' \cdot \mathbf{t}_2), \theta, \phi, \psi)$.

The impact parameter $\delta = \mathbf{X}_0^\perp$ has to be chosen randomly at each scattering. The impact parameter has two dof. One is the absolute value δ and another is the angular coordinate θ_X . Then

$$\mathbf{X}_0^\perp = \delta [\cos \theta_X \mathbf{s}_1 + \sin \theta_X \mathbf{s}_2]. \quad (\text{B.12})$$

Performing a 2-dimensional coordinate transformation,

$$\begin{pmatrix} \mathbf{s}_1 \\ \mathbf{s}_2 \end{pmatrix} = \begin{pmatrix} \cos \chi & \sin \chi \\ -\sin \chi & \cos \chi \end{pmatrix} \begin{pmatrix} \tilde{\mathbf{s}}_1 \\ \tilde{\mathbf{s}}_2 \end{pmatrix}, \quad (\text{B.13})$$

the impact parameter \mathbf{X}_0^\perp can be expressed as

$$\mathbf{X}_0^\perp = \delta [\cos(\theta_X + \chi) \tilde{\mathbf{s}}_1 + \sin(\theta_X + \chi) \tilde{\mathbf{s}}_2]. \quad (\text{B.14})$$

Therefore, by using the dof for the rotation of the 2-dimensional coordinate basis the angular dof θ_X can be chosen freely. We set $\theta_X = \pi/2$.

For the distribution of δ , from its definition we set $P(\delta)d\delta \propto \delta d\delta$ with the cutoff at $\delta = \xi/a$. Then we fix the range of integration $X^\perp(\sigma) \leq \xi/a$ for a given δ . For a string segment with the parabola-type shape, Eq. (4.2), the condition can be written as

$$a_0 - \frac{\xi^2}{a^2} + a_1\sigma + a_2\sigma^2 + a_3\sigma^3 \leq 0. \quad (\text{B.15})$$

For a given value of the impact parameter at $\delta \leq \xi/a$, the range of σ is chosen to satisfy the above equation.

For the angular variables θ , ϕ and ψ , we choose uniform distributions $P(\cos\theta) = 1/2$, $P(\phi) = P(\psi) = 1/2\pi$. As for v , we fix it at $v = v_{\text{rms}}$ for simplicity.

We fix the value of $(\mathbf{r}_0'' \cdot \mathbf{t}_1)$ by using Eq. (4.5) so that it is consistent with the correlation between the string velocity and the curvature. As for the remaining three dof, we set $(\mathbf{r}_0'' \cdot \mathbf{t}_2) = 0$, $(\dot{\mathbf{r}}_0' \cdot \mathbf{t}_1) = 0$ and $(\dot{\mathbf{r}}_0' \cdot \mathbf{t}_2) = 0$. Note that this is solely due to the lack of our knowledge about the curvature and rotation of string segments.

References

- [1] A. A. Fraisse, C. Ringeval, D. N. Spergel and F. R. Bouchet, Phys. Rev. D **78**, 043535 (2008) [arXiv:0708.1162 [astro-ph]].
- [2] R. Jeannerot, J. Rocher and M. Sakellariadou, Phys. Rev. D **68**, 103514 (2003) [arXiv:hep-ph/0308134].
- [3] S. Sarangi and S. -H. H. Tye, Phys. Lett. B **536**, 185 (2002) [arXiv:hep-th/0204074].
- [4] A. -C. Davis and T. W. B. Kibble, Contemp. Phys. **46**, 313 (2005) [arXiv:hep-th/0505050].
- [5] E. J. Copeland and T. W. B. Kibble, arXiv:0911.1345 [hep-th].
- [6] M. Majumdar, arXiv:hep-th/0512062.
- [7] M. G. Jackson, N. T. Jones and J. Polchinski, JHEP **0510**, 013 (2005) [arXiv:hep-th/0405229].
- [8] M. Eto, K. Hashimoto, G. Marmorini, M. Nitta, K. Ohashi and W. Vinci, Phys. Rev. Lett. **98**, 091602 (2007) [arXiv:hep-th/0609214].
- [9] P. Salmi, A. Achúcarro, E. J. Copeland, T. W. B. Kibble, R. de Putter and D. A. Steer, Phys. Rev. D **77**, 041701 (2008) [arXiv:0712.1204 [hep-th]].
- [10] L. Pogosian, S. -H. Tye, I. Wasserman and M. Wyman, JCAP **0902**, 013 (2009) [arXiv:0804.0810 [astro-ph]].
- [11] N. Bevis, M. Hindmarsh, M. Kunz and J. Urrestilla, Phys. Rev. Lett. **100**, 021301 (2008) [arXiv:astro-ph/0702223].
- [12] L. Pogosian, S. H. -H. Tye, I. Wasserman and M. Wyman, Phys. Rev. D **68**, 023506 (2003) [Erratum-ibid. D **73**, 089904 (2006)] [arXiv:hep-th/0304188].
- [13] L. Perivolaropoulos, Nucl. Phys. Proc. Suppl. **148**, 128 (2005) [arXiv:astro-ph/0501590].
- [14] J. E. Ruhl *et al.* [The SPT Collaboration], Proc. SPIE Int. Soc. Opt. Eng. **5498**, 11 (2004) [arXiv:astro-ph/0411122].
- [15] A. Kosowsky, New Astron. Rev. **47**, 939 (2003) [arXiv:astro-ph/0402234].

- [16] N. Kaiser and A. Stebbins, *Nature* **310** (1984) 391.
- [17] J. R. I. Gott, *Astrophys. J.* **288**, 422 (1985).
- [18] E. Komatsu and D. N. Spergel, *Phys. Rev. D* **63**, 063002 (2001) [arXiv:astro-ph/0005036].
- [19] A. Gangui, L. Pogosian and S. Winitzki, *Phys. Rev. D* **64**, 043001 (2001) [arXiv:astro-ph/0101453].
- [20] M. Hindmarsh, C. Ringeval and T. Suyama, arXiv:0908.0432 [astro-ph.CO].
- [21] M. Hindmarsh, C. Ringeval and T. Suyama, arXiv:0911.1241 [astro-ph.CO].
- [22] D. M. Regan and E. P. S. Shellard, arXiv:0911.2491 [astro-ph.CO].
- [23] M. Hindmarsh, *Astrophys. J.* **431**, 534 (1994) [arXiv:astro-ph/9307040].
- [24] K. Takahashi, A. Naruko, Y. Sendouda, D. Yamauchi, C. -M. Yoo and M. Sasaki, *JCAP* **0910**, 003 (2009) [arXiv:0811.4698 [astro-ph]].
- [25] C. J. A. Martins and E. P. S. Shellard, *Phys. Rev. D* **65**, 043514 (2002) [arXiv:hep-ph/0003298].
- [26] C. J. A. Martins and E. P. S. Shellard, *Phys. Rev. D* **54**, 2535 (1996) [arXiv:hep-ph/9602271].
- [27] A. Avgoustidis and E. P. S. Shellard, *Phys. Rev. D* **73**, 041301 (2006) [arXiv:astro-ph/0512582].
- [28] A. Stebbins and S. Veeraraghavan, *Phys. Rev. D* **51**, 1465 (1995) [arXiv:astro-ph/9406067].
- [29] A. Stebbins, *Astrophys. J.* **327**, 584 (1988).
- [30] A. Vilenkin and E. P. S. Shellard, *Cosmic Strings and Other Topological Defects* (Cambridge University Press, Cambridge, England, 1994)
- [31] T. W. B. Kibble, *Nucl. Phys. B* **252**, 227 (1985) [Erratum-ibid. B **261**, 750 (1985)].
- [32] C. Ringeval, M. Sakellariadou and F. Bouchet, *JCAP* **0702**, 023 (2007) [arXiv:astro-ph/0511646].
- [33] C. J. A. Martins, J. N. Moore and E. P. S. Shellard, *Phys. Rev. Lett.* **92**, 251601 (2004) [arXiv:hep-ph/0310255].
- [34] L. Cayon, E. Martinez-Gonzalez, F. Argueso, A. J. Banday and K. M. Gorski, *Mon. Not. Roy. Astron. Soc.* **339**, 1189 (2003) [arXiv:astro-ph/0211399].
- [35] D. Yamauchi, C. -M. Yoo, K. Takahashi, Y. Sendouda, A. Naruko, and M. Sasaki, in preparation